Impact of nanofiber coatings on the air permeability and pressure drop of nonwoven filter media

Nitin A. Charhate, Bhushan B. Chaudhari and Tushar D. Deshpande*

University Institute of Chemical Technology, K.B.C. North Maharashtra University, Jalgaon-425001 (M.S.), INDIA

Corresponding author: Dr. Tushar D. Deshpande

Abstract

Growing global concern over airborne particulate matter ($PM_{2.5}$) is driving the search for advanced air filtration materials that can deliver high efficiency without the environmental and economic drawbacks of conventional single-use filters. In this study, we developed and assessed a composite filter medium intended for reusable applications. Using a high-throughput, needleless electrospinning technique, we deposited a functional nanofibre layer of polyamide 6 (PA6) and polyvinylidene fluoride (PVDF) onto a robust PET bicomponent spunbond substrate. The aim was to systematically evaluate how this nanofibre coating influences the filter's morphology and aerodynamic performance.

Scanning Electron Microscopy (SEM) confirmed the successful formation of a uniform, defect-free nanofibre web, with average fibre diameters ranging from 150 to 180 nm. Performance testing revealed a marked change in the medium's aerodynamic characteristics: the addition of the nanofibre layer reduced air permeability by up to 73% and increased the pressure drop by as much as 340% in multi-layer configurations, compared with the uncoated substrate. These results clearly illustrate the inherent trade-off between improved particle capture—driven by the dense nanofibre structure—and the accompanying rise in airflow resistance.

This work provides a valuable dataset and a sound basis for the design and optimisation of next-generation filter media, where filtration efficiency, energy consumption and breathability must be carefully balanced to meet the demands of advanced air purification systems.

1. Introduction

The growing problem of air pollution—particularly the widespread presence of fine particulate matter ($PM_{2.5}$)—has emerged as one of the most pressing environmental health challenges of the 21st century. These microscopic particles, generated by industrial emissions, vehicle

exhaust, and other human activities, are small enough to penetrate deep into the respiratory system. Prolonged exposure is linked to a range of serious health effects, including cardiovascular disease, respiratory disorders, and a reduction in overall life expectancy (Cohen et al., 2017). Consequently, the need for high-performance air filtration technologies—capable of effectively removing harmful pollutants from both ambient and indoor air—has never been more urgent. Conventional systems, such as High-Efficiency Particulate Air (HEPA) filters, have long been regarded as the benchmark for particle removal. Typically composed of randomly oriented glass or polymer microfibres, these filters can deliver exceptionally high capture efficiencies. However, this performance comes at a cost: the dense, thick structures required to achieve such efficiency result in a significant pressure drop, thereby increasing the energy demands of air-handling systems. In addition, most conventional filter media are designed for single use, necessitating frequent replacement, incurring high operational costs, and contributing to substantial environmental impacts through waste generation(Kumar et al., 2023; P. Li et al., 2014; Singh et al., 2024; Zhu et al., 2017). This situation underscores the urgent need for advanced filtration materials that can achieve an optimal balance between efficiency, energy consumption, and sustainability. Addressing these demands, electrospun nanofibre membranes have emerged as a highly promising next-generation filtration technology. Electrospinning is a versatile and effective method for producing polymer fibres with diameters typically ranging from 50 to 500 nm. The resulting nanofibre mats exhibit an exceptionally high surface-area-to-volume ratio, small inter-fibre pore sizes, and high porosity—properties that are particularly advantageous for capturing fine particulate matter while maintaining relatively low airflow resistance(Bhardwaj et al., 2010). These intrinsic properties enable nanofibre-based filters to capture fine particles with outstanding efficiency through mechanisms such as interception and diffusion. Furthermore, the “slip flow” effect at the nanofibre surface allows these materials to maintain high capture efficiency while generating a comparatively moderate pressure drop. This characteristic not only improves airflow but also offers the potential for substantial energy savings when compared with conventional microfibre-based filters(Ahn et al., 2006). An especially effective approach involves producing a composite filter medium by depositing a thin, functional nanofibre layer onto a robust, low-cost conventional nonwoven substrate. This design combines the mechanical strength and structural stability of the substrate with the enhanced filtration performance of the nanofibre coating. The primary aim of this study is to fabricate such a composite medium using a scalable, high-throughput needleless electrospinning technique. In particular, we explore the coating of a polyethylene terephthalate (PET) bicomponent spunbond substrate with polyamide

6 (PA6) and polyvinylidene fluoride (PVDF) nanofibres. The work focuses on systematically evaluating the morphological and aerodynamic changes introduced by this modification. By precisely characterising air permeability and pressure drop before and after coating, this research delivers a quantitative assessment of the performance trade-offs involved in developing next-generation, high-efficiency, and potentially reusable air filters.

2. Material and Methods

2.1. Materials

2.1.1. Polymers

The primary polymers selected for fabricating the nanofibre membranes in this study were polyamide 6 (PA6), supplied by BASF, and polyvinylidene fluoride (PVDF), sourced from Arkema. This choice was intentional, based on their well-documented properties that are highly advantageous for advanced air filtration applications. Several performance factors underpin this selection, particularly in the context of developing high-efficiency, reusable filter media: a) Filtration efficiency - Both PA6 and PVDF are highly compatible with the electrospinning process, enabling the production of uniform nanofibres with sub-micron diameters. The resulting high surface-area-to-volume ratio and dense fibrous network are critical for capturing fine and ultrafine particulate matter ($PM_{2.5}$ and smaller) through enhanced interception and diffusion mechanisms. Literature reports indicate that composite PA6/PVDF filters can achieve efficiencies exceeding 99%, with PA6/PVDF-10 composite mats delivering 93% efficiency at a pressure drop of 194 Pa. More recent studies have shown that PVDF-based filters can reach efficiencies of up to 99.57% for fine particles(Sanyal 2025).

Mechanical and chemical robustness – For a filter to be genuinely reusable, it must endure repeated cleaning cycles without significant loss of performance. PA6 provides excellent mechanical strength and tensile properties, ensuring structural integrity and durability of the nanofibre layer and reducing the risk of damage during handling or washing. PVDF offers exceptional chemical inertness and thermal stability, allowing the filter medium to maintain its performance even after exposure to cleaning agents or environmental stressors. When combined, these materials produce composite filters with both superior mechanical resilience and outstanding filtration performance. For example, PVDF/PA6 composite membranes have been reported to achieve efficiencies as high as 99.5%, while maintaining manageable pressure drops(Venkataraman, 2024) (Luo et al. 2024.) Airflow dynamics (breathability) – While high filtration efficiency is essential, it must not come at the expense of excessive airflow resistance.

Nanofibrous structures produced from PA6 and PVDF inherently exhibit high porosity, which promotes optimal air permeability while sustaining effective particle capture. This balance between breathability and efficiency is critical for both energy efficiency and user comfort. Furthermore, surface modification techniques such as corona discharge treatment have been shown to enhance the filtration quality factor of PVDF-based filters by up to 60%, without compromising airflow performance.(Sanyal & Sinha-Ray, 2021).

2.1.2. Solvents

To prepare the polymer solutions for electrospinning, a suite of analytical-grade solvents was used, including formic acid, acetic acid, dimethylacetamide (DMAc), and dimethylformamide (DMF), all procured from certified suppliers in India. The choice of this solvent system was critical to producing homogeneous polymer solutions with the optimal viscosity, surface tension, and electrical conductivity required for stable and continuous electrospinning. For PA6, a mixture of formic acid and acetic acid in a 4:1 weight ratio has been widely recognised as an effective solvent system. In this formulation, formic acid acts as the primary solvent for PA6, while acetic acid raises the boiling point of the mixture and enhances spinnability. This combination has been shown to produce uniform nanofibres with average diameters as small as 83.5 nm. Recent studies further confirm that PA6 solutions prepared in 85% formic acid yield continuous, defect-free electrospun fibres, whereas alternative solvent systems frequently lead to structural imperfections.(Chidchanok Mit-uppatham, et al.)

For PVDF, solvents such as DMF and DMAc—often blended with acetone—are widely employed to produce spinnable solutions that yield uniform, defect-free fibres. Among these, a DMF/acetone mixture in a 6:4 ratio has proven particularly effective in generating PVDF nanofibres with controlled morphology and diameter. The choice of solvent has a pronounced effect on fibre characteristics: for instance, DMAc/acetone systems typically produce fibres with diameters of around 352.9 ± 24 nm, whereas DMF/acetone systems result in larger diameters of approximately 611.9 ± 27 nm. In addition, dimethyl sulfoxide (DMSO) has recently emerged as a promising, low-toxicity alternative to traditional solvents for PVDF electrospinning, offering potential benefits in terms of safety and environmental impact(Motamedi et al., 2017a).

2.1.3. Substrate Selection

A polyethylene terephthalate (PET) bicomponent spunbond nonwoven fabric was selected as the base substrate. The choice was guided by key parameters influencing both electrospinning performance and the final characteristics of the composite filter medium. Internal volume and surface resistivity were assessed to ensure efficient charge transfer during electrospinning, enabling uniform nanofibre formation. Appropriate resistivity levels facilitate effective charge dissipation and minimise fibre repulsion during deposition shows electrical properties(Heng et al., 2015). Physical properties such as substrate's basis weight (GSM), air permeability, and baseline pressure drop were characterised to determine optimal processing configurations. The PET bicomponent structure—comprising a PET core encased in a polyethylene (PE) sheath—offers high mechanical strength and smooth handling, which are essential for industrial-scale filtration applications. This bicomponent architecture also provides thermal bonding and heat lamination capabilities, making it suitable not only for air filtration but also for packaging and technical textile applications. Crucially, it delivers the structural stability required to support the delicate nanofibre coating without compromising performance (Khawar et al., 2023)..

2.1.4. Needleless Electrospinning Apparatus and Procedure

The nanofibre coatings were fabricated using a custom-built, high-throughput needleless electrospinning system, chosen over conventional needle-based methods for its superior scalability and ability to produce large, uniform nanofibre mats—an essential requirement for industrial filter media production. The system comprises several key components, each precisely controlled to ensure consistent and reproducible nanofibre formation with the desired morphological characteristics. This approach enables the efficient production of high-quality coatings suitable for large-scale applications while maintaining the fine structural control required for advanced filtration performance(Bokka, 2022; Sedar, 2025).

2.1.4.1. Spinneret Design

At the heart of the needleless electrospinning system is the spinneret, which generates multiple polymer jets simultaneously from a free liquid surface. The spinneret's design is critical, as it directly influences both the production rate and fibre uniformity. Drawing on insights from recent reviews of high-throughput electrospinning technologies ((Yu et al., 2017)), our system was engineered to support a range of spinneret configurations. For this study, a rotating cylinder spinneret was selected as the primary configuration, offering a reliable balance between output capacity and fibre quality. Rotating cylinder/disc spinneret – This configuration consists of a rotating metal cylinder partially immersed in a reservoir of the polymer solution. A high

electrical potential is applied to the cylinder, inducing charge accumulation at the surface of the solution. As the cylinder rotates, it lifts a thin film of the solution upward, where the intense electric field overcomes surface tension, leading to the formation of multiple Taylor cones and the subsequent ejection of polymer jets. This approach is highly effective for large-scale production of nanofibres, although it offers limited control over precise fibre alignment(Teo & Ramakrishna, 2006). Other needleless electrospinning designs reported in the literature include wire electrodes and free-surface configurations, both of which operate on the principle of generating a large, charged surface area to maximise nanofibre yield.

2.1.4.2. High Voltage Power Supply

A high-voltage DC power supply generates the electric field required for electrospinning, with applied voltages typically in the range of 10–30 kV. This parameter is critical, as it directly affects fibre initiation, formation, and morphology. The voltage must be carefully optimised: if too low, it will be insufficient to overcome the surface tension of the polymer solution, preventing jet initiation; if too high, it can cause electrical discharge, jet instability, and a wider distribution of fibre diameters, often resulting in beaded or defective fibres(Deitzel et al., 2001).

2.1.4.3. Polymer Solution Flow Rate

In needleless electrospinning systems, maintaining a consistent supply of polymer solution to the spinneret is essential for stable operation. The replenishment rate of the solution in the reservoir directly influences both fibre diameter and process stability. A lower replenishment rate generally promotes the formation of thinner fibres due to greater jet stretching; however, if it is too low, the supply becomes insufficient, interrupting continuous fibre formation. Conversely, a higher replenishment rate can enhance production throughput and yield thicker fibres, but excessive rates may lead to dripping and process instability(Reneker & Yarin, 2008).

2.1.4.4. Nanofiber Collection Method

The final structure and properties of nanofibre filter media are strongly influenced by the collection method. The collector serves as a grounded target on which solidified nanofibres are deposited. While a simple stationary metal plate can be used to produce a randomly oriented non-woven mat, this study employed a rotating drum collector. In this method, a cylindrical drum rotates at a controlled speed, with its high surface velocity imparting a mechanical drawing force on the incoming nanofibres prior to deposition. This results in partial fibre

alignment parallel to the direction of rotation. The rotation speed and drum diameter are critical parameters governing the degree of fibre orientation, packing density, and anisotropy in the final nanofibre mat(Grasl et al., 2013).

2.1.4.5. Environmental Control

The electrospinning process is highly sensitive to ambient environmental conditions; therefore, the entire setup was enclosed within a controlled chamber to maintain stable temperature and humidity, ensuring process stability and reproducibility. Temperature: Ambient temperature influences both the viscosity of the polymer solution and the solvent evaporation rate. Maintaining a consistent temperature is essential for preserving uniform solution properties and achieving predictable fibre formation. Humidity: Relative humidity affects solvent evaporation and can significantly influence fibre morphology. Elevated humidity may slow solvent evaporation, resulting in beaded fibres or incomplete solidification. For polymers sensitive to moisture, precise humidity control is critical to avoid undesirable surface morphologies or structural defects(Casasola et al., 2016).

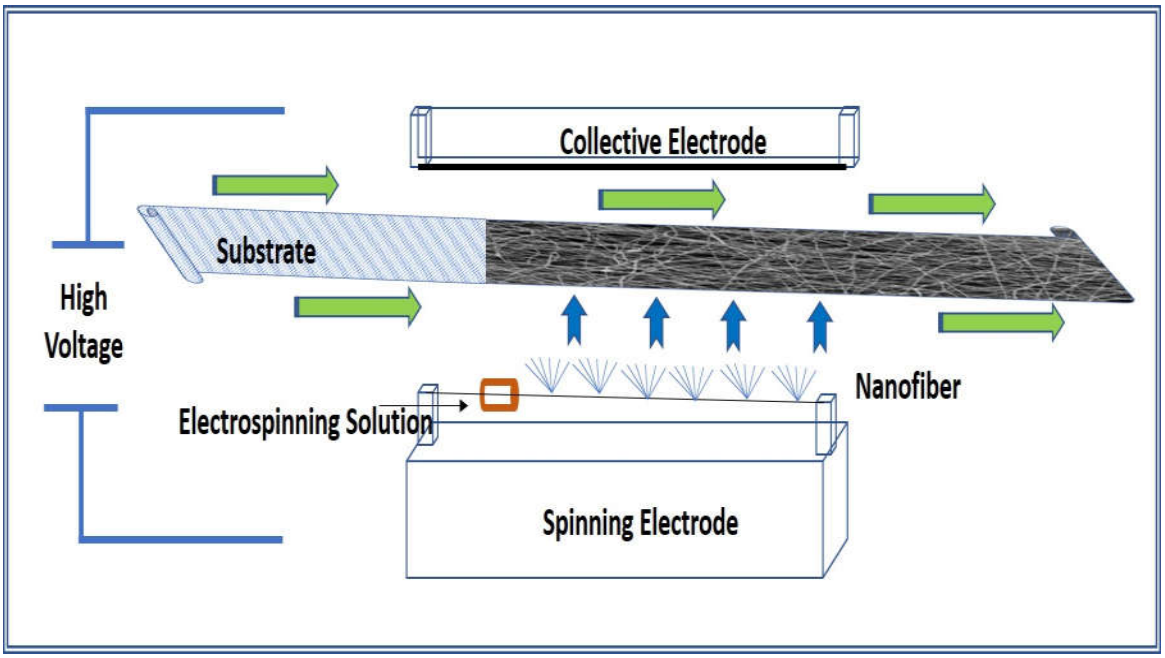

Fig.1. Needleless electrospinning technology schematic diagram

2.2. Experimental Procedure for Filter Media Fabrication and Evaluation

The development of the composite nanofiber filter media followed a systematic, multi-stage approach aimed at maximizing performance, beginning with the selection of the most suitable

base media and configuration, and subsequently applying and characterizing the functional nanofiber coating to achieve the desired filtration properties.

2.2.1. Baseline Characterization and Selection of Substrate Media

The initial phase focused on selecting the most suitable substrate material to serve as the mechanical support for the nanofiber layer. A range of PET bicomponent spunbond nonwoven fabrics with varying GSM values were procured and comprehensively characterized to establish baseline performance metrics, with air permeability (ASTM D737) and pressure drop as the primary evaluation parameters. This screening identified substrates offering an optimal balance of low airflow resistance and sufficient structural integrity. Based on the optimal GSM range, the selected base media were prepared in single-layer and two-layer configurations, which were then tested for air permeability and pressure drop to determine the most effective layering strategy. The configuration demonstrating the most favorable aerodynamic performance was subsequently selected for the nanofiber coating stage.

2.2.2. Application of Nanofiber Coating via Needleless Electrospinning

The optimized single-layer and two-layer substrate configurations were coated with PA6/PVDF nanofibers using the needleless electrospinning apparatus described in Section 2.1. The process parameters—including applied voltage, polymer solution concentration, and environmental conditions—were meticulously controlled to ensure the deposition of a uniform, defect-free nanofiber layer with the desired fiber diameter and morphology across the entire surface of the substrate (Gibson et al., 2001). The primary objective of this step was to impart a high-efficiency particulate capture capability to the base media.

2.2.3. Post-Treatment via Thermal Calendering

Following electrospinning, the nanofiber-coated samples underwent thermal calendering, wherein they were passed between two heated rollers under controlled temperature and pressure to enhance the durability and performance of the composite media. This post-treatment step served to improve interfacial adhesion between the delicate nanofiber layer and the substrate, thereby preventing delamination during handling or cleaning, and to consolidate the nanofiber mat, improving its mechanical strength and stability. The process conditions were carefully optimized to maximize bond strength while preserving the fibrous structure and avoiding excessive increases in pressure drop.

2.2.4. Final Performance Characterization of Composite Filter Media

The final, post-treated composite filter media, prepared in both single- and two-layer configurations, underwent a concluding series of performance evaluations. Air permeability and pressure drop measurements were repeated, enabling a direct, quantitative comparison with the baseline data obtained from the uncoated substrates. This final characterization provided a precise assessment of the nanofiber coating and post-treatment effects on the filter's aerodynamic performance, thereby validating the overall effectiveness of the fabrication process.

3. Characterization and Performance Evaluation

3.1. Morphological Characterization

The primary aim of the morphological characterisation was to visually examine the nanofibre structure and to quantitatively evaluate key physical parameters, including fibre diameter and uniformity, as these have a direct and significant influence on filtration performance.

3.1.1. Scanning Electron Microscopy (SEM)

The surface morphology of the electrospun Polyamide 6 (PA6), Polyvinylidene fluoride (PVDF), and composite nanofibre layers, along with the underlying PET bicomponent substrate, was examined using a high-resolution Scanning Electron Microscope (SEM). Sample preparation prior to imaging includes, small sections of the filter media were carefully mounted onto aluminium stubs using double-sided conductive carbon tape. To prevent electrostatic charging under the electron beam and to enhance image clarity, the samples were sputter-coated with a thin layer (approximately 5–10 nm) of gold or platinum. This standard procedure ensures high-resolution, well-defined images of the non-conductive polymer fibres(Širc et al., 2012). The SEM was operated at an accelerating voltage optimised for delicate polymer structures (typically 5–15 kV). The resulting micrographs provided essential qualitative insights into:

- Fibre uniformity: Evaluating the consistency of the nanofibre mat across the substrate.
- Fibre morphology: Identifying any defects such as beads, branching, or fused fibres, which could impair performance.
- Surface coverage: Assessing the density and uniformity of the nanofibre coating on the substrate.

3.2. Fiber Diameter Distribution

A quantitative analysis of nanofibre diameter was performed to develop a statistical understanding of fibre size, a critical factor influencing both filtration efficiency and pressure drop. Measurement technique: High-magnification SEM images were analysed using the open-source image analysis software ImageJ (or Fiji). For each sample type (PA6 and PVDF), a statistically significant number of fibres (typically $n > 100$) were randomly selected from multiple micrographs to ensure a representative dataset(Schneider et al., 2012). Data analysis: The measured diameters were used to construct fibre diameter distribution histograms, providing a visual representation of the size range and uniformity of the electrospun fibres. Key statistical descriptors, including the mean fibre diameter and standard deviation, were calculated to deliver a concise quantitative summary of the fibre morphology.

3.3. Performance Evaluation: Aerodynamic Properties

The aerodynamic performance of the fabricated filter media is a critical determinant of its suitability for air purification applications. The two primary metrics evaluated were air permeability, which indicates the ease with which air can pass through the material, and pressure drop, which quantifies the resistance to airflow. These properties were meticulously measured to assess the impact of the nanofiber coating on the substrate's performance

3.3.1. Air Permeability Testing

The air permeability of both the uncoated substrates and the final composite nanofibre media was measured in strict accordance with ASTM D737-18, using a dedicated air permeability tester. Circular specimens were clamped into the test head, and a constant pressure differential of 125 Pa (equivalent to 12.7 mm of water) was applied across a defined test area of 38.5 cm^2. The instrument recorded the airflow rate (in L/min or ft^3/min) required to maintain this pressure drop. All samples were conditioned for at least 24 hours in a standard atmosphere of 21 ± 1 °C and 65 ± 2 % relative humidity to ensure consistency and eliminate environmental influences. Care was taken to mount specimens flat and without wrinkles or tension to avoid artefacts in the results. Air permeability (P) was calculated by normalising the measured airflow rate by the test area and expressed in units of L/m^2/s or ft^3/min/ft^2, enabling direct comparison across different samples. Although parameters such as temperature, humidity, and sample thickness can affect measurements, strict adherence to the standard conditioning and testing protocols minimised their impact, ensuring reliable and reproducible data(Motamedi et al., 2017b).

3.3.2. Pressure Drop Measurement

Pressure drop, also referred to as differential pressure, represents the resistance that the filter media presents to airflow at a given face velocity. This parameter is critical, as it directly affects the energy consumption of an air purification system. Pressure drop was measured using a custom-built air filter test rig, following the principles set out in standards such as ASHRAE 52.2 and ISO 16890. While EN 779 provides a classification framework for filters, ISO 16890 offers a more comprehensive procedural guide, which was adopted for this study (Aruchamy et al., n.d.). Testing was carried out by maintaining a constant airflow rate through the filter specimen, corresponding to a face velocity representative of typical air purifier operation (e.g., 0.1–1.5 m/s). The airflow was generated by a calibrated fan and precisely regulated using a mass flow controller to ensure stability throughout the measurement. The pressure differential between the upstream and downstream sides of the filter was measured using a high-precision digital manometer, with an accuracy of ±0.1 Pa across the measurement range. This ensured highly reliable readings of the filter's resistance. Pressure drop is strongly influenced by face velocity, with resistance increasing as airflow speed rises. Other contributing factors include the total filter surface area and the properties of the air (such as density and viscosity). All measurements were conducted under controlled conditions to enable a direct and fair comparison between the uncoated substrates and the nanofibre-coated media.

4. Results and Discussion

4.1. Morphological Analysis of Nanofiber Layers (SEM)

4.1.1. Visual Characterization

Scanning Electron Microscopy (SEM) was used to visualize the surface morphology of the electrospun PA6 and PVDF nanofibers on the PET bicomponent substrate.

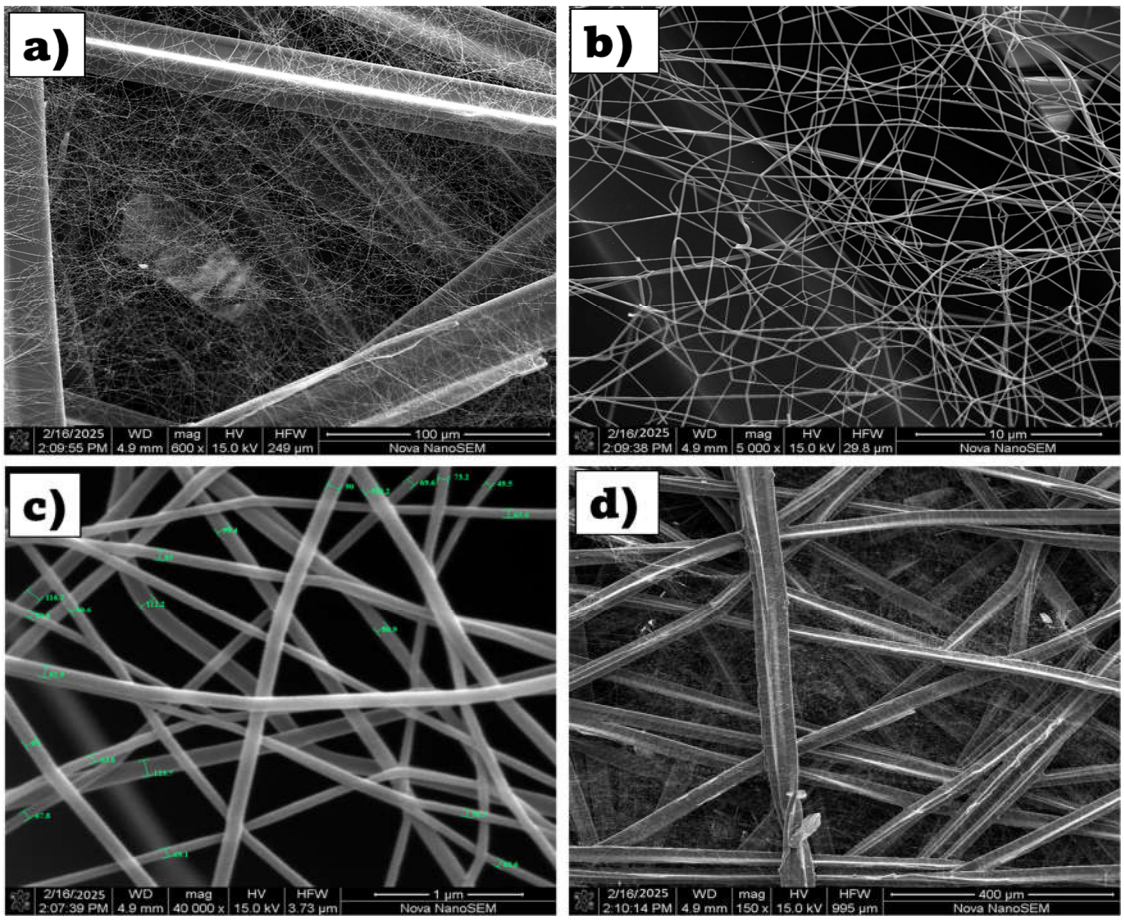

Figure 1SEM micrographs of electrospun PA6 nanofibre media at different magnifications

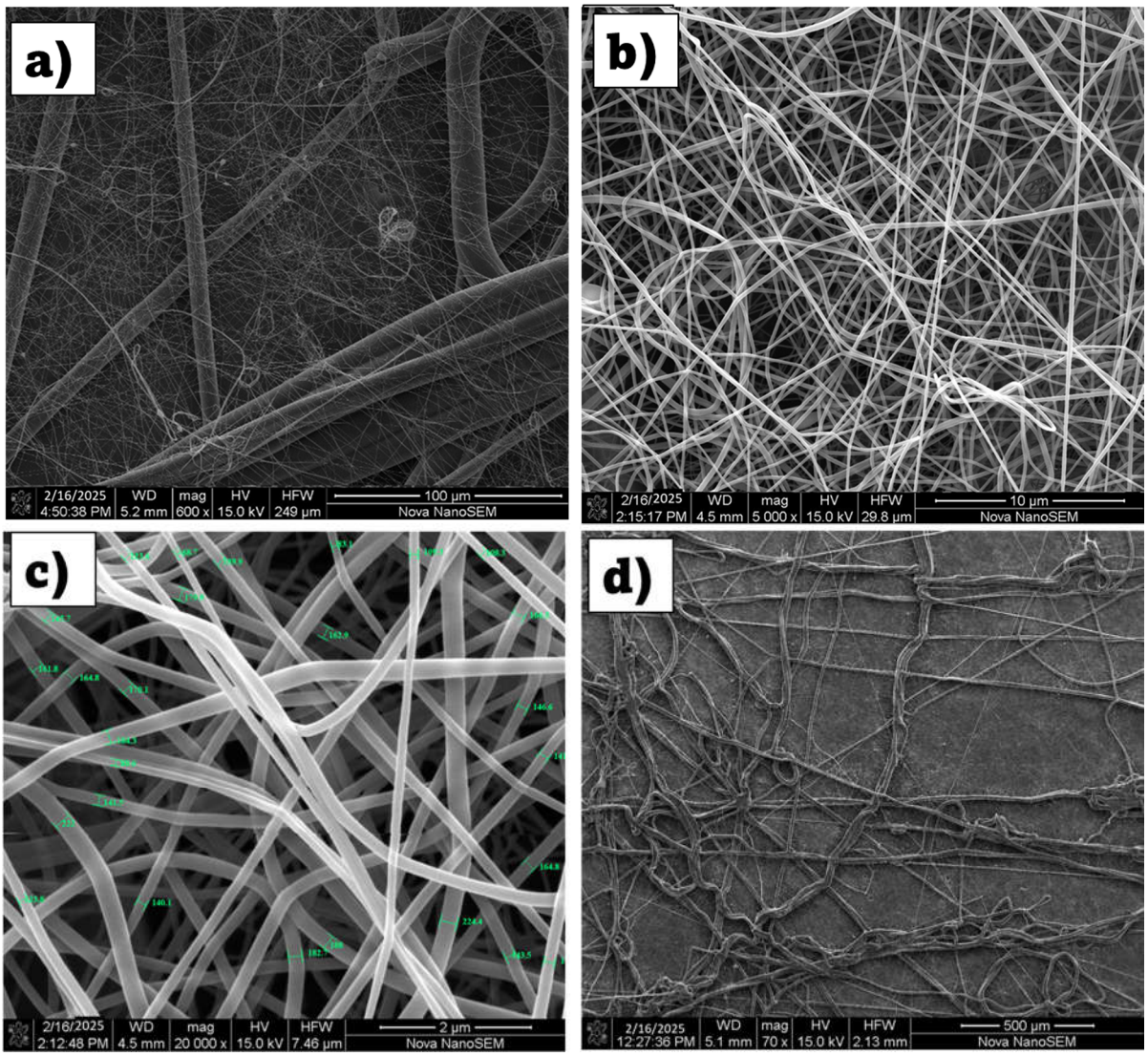

Figure 2 SEM micrographs of electrospun PVDF nanofibre media at varying magnifications

The SEM micrographs in Figure 1 and Figure 2 confirmed that the needleless electrospinning process successfully yielded a uniform and densely packed nanofibre web for both Polyamide 6 (PA6) and Polyvinylidene fluoride (PVDF), fully covering the underlying substrate. At low magnification, the PVDF nanofibres (Figure 2a, 2d) and PA6 nanofibres formed continuous, well-distributed layers over the base media, with the coarser support fibres partially visible beneath. Higher magnification views (Figure 2b) revealed an interconnected, random network with smooth, bead-free morphology for both materials, indicating stable jet formation during electrospinning. Ultra-high magnification analysis (Figure 2c) demonstrated that the PVDF fibres exhibited a narrow diameter distribution in the sub-micrometre range (~140–260 nm), while PA6 fibres displayed similarly consistent diameters within their respective ranges,

reflecting precise process control. This structural uniformity is essential for ensuring reproducible air permeability and filtration efficiency.

The presence of the nanofibre coating significantly reduced the apparent pore size of the base substrate, producing a tortuous airflow path critical for fine particulate capture. In both PA6- and PVDF-coated media, the smooth surface morphology and uniform fibre deposition are expected to minimise defects such as beading or fused junctions, which could otherwise compromise filtration performance. The hierarchical structure—comprising a mechanically robust microfibre substrate overlaid with an ultrafine nanofibre mat—combines strength with enhanced filtration capability. Such architecture not only increases the surface area-to-volume ratio but also facilitates effective interception, diffusion, and electrostatic capture mechanisms, thereby improving the overall efficiency of airborne particle removal without imposing excessive pressure drop.

4.1.2. Fiber Diameter Distribution

Quantitative analysis of the SEM micrographs was conducted using ImageJ image analysis software(Schneider et al., 2012.) to determine the fiber diameter distributions for both nanofiber types. For PA6 nanofibers, the mean diameter was measured at 150 ± 30 nm, while PVDF nanofibers exhibited a slightly larger average of 180 ± 40 nm. In both cases, the relatively narrow standard deviations indicate a tight clustering of diameters around the mean, reflecting the high degree of control maintained over the electrospinning parameters, including polymer solution concentration, applied voltage, spinneret–collector distance, and environmental humidity.

Achieving such uniform fiber dimensions is essential for consistent filter performance, as fiber diameter strongly influences filtration efficiency, pressure drop, and the balance between particle capture and air permeability (Huang et al., 2020). Specifically, nanofibers within the sub-micrometer range offer a high specific surface area, which enhances interception and diffusion-based capture of fine particles, while their narrow size distribution helps ensure predictable and reproducible performance across filter batches. This level of morphological control aligns with previous reports that link electrospinning precision to enhanced air filtration efficiency without significantly increasing resistance to airflow (Cho et al., 2025).

4.2. Aerodynamic Performance

4.2.1. Air Permeability

Air permeability was measured according to ASTM D737 to quantify the ease of airflow through the media. The results for single-layer and two-layer configurations are presented below.

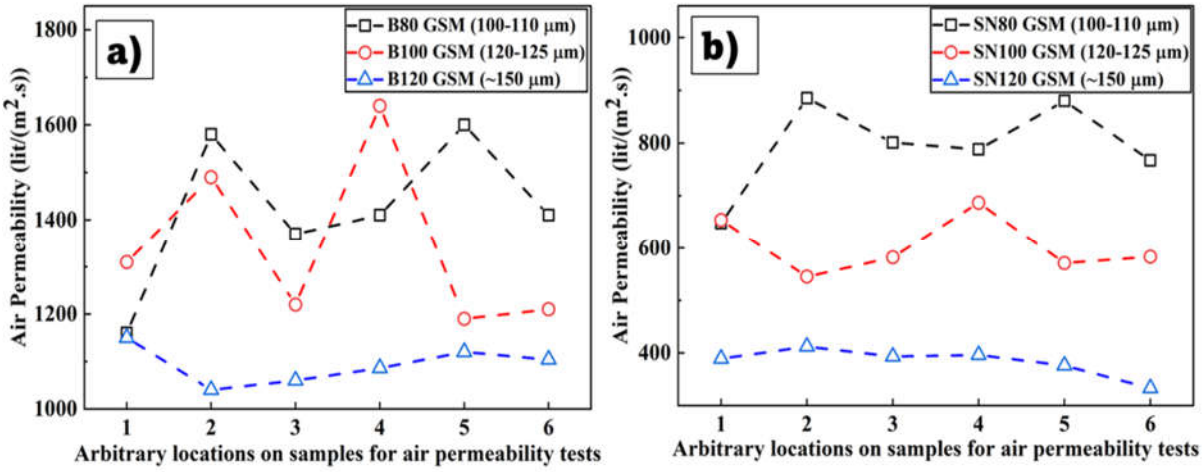

Figure 3 Air Permeability Performance of Nanofiber uncoated (a) and Coated (b)Substrates

Substrate GSM	Avg. Air Permeability of Blank Substrate (L/m²/s)	Avg. Air Permeability of Coated Substrate (L/m²/s)	Percent Reduction in Permeability (%)
80	1422 ± 165.7	795 ± 98.4	44.1
100	1343 ± 179.6	604 ± 61.1	55.0
120	1093 ± 46.2	383 ± 27.8	64.9

Table 1 Air Permeability Performance of Nanofiber uncoated and Coated Substrates

The results presented in Figure 3(a,b) and the corresponding quantitative data clearly indicate that the application of electrospun nanofiber layers leads to a substantial reduction in air permeability across all tested substrate grammages (GSM). For the uncoated substrates, the average air permeability ranged from 1422 ± 165.7 L/m²/s for 80 GSM to 1093 ± 46.2 L/m²/s for 120 GSM, reflecting the inherent differences in base media porosity. Upon deposition of the nanofiber coating, permeability values dropped significantly—to 795 ± 98.4 L/m²/s (80 GSM), 604 ± 61.1 L/m²/s (100 GSM), and 383 ± 27.8 L/m²/s (120 GSM)—corresponding to reductions of 44.1%, 55.0%, and 64.9%, respectively. This trend aligns with the understanding

that higher GSM substrates inherently possess smaller pore structures, thereby amplifying the impact of nanofiber deposition on airflow resistance (X. Li et al., 2025).

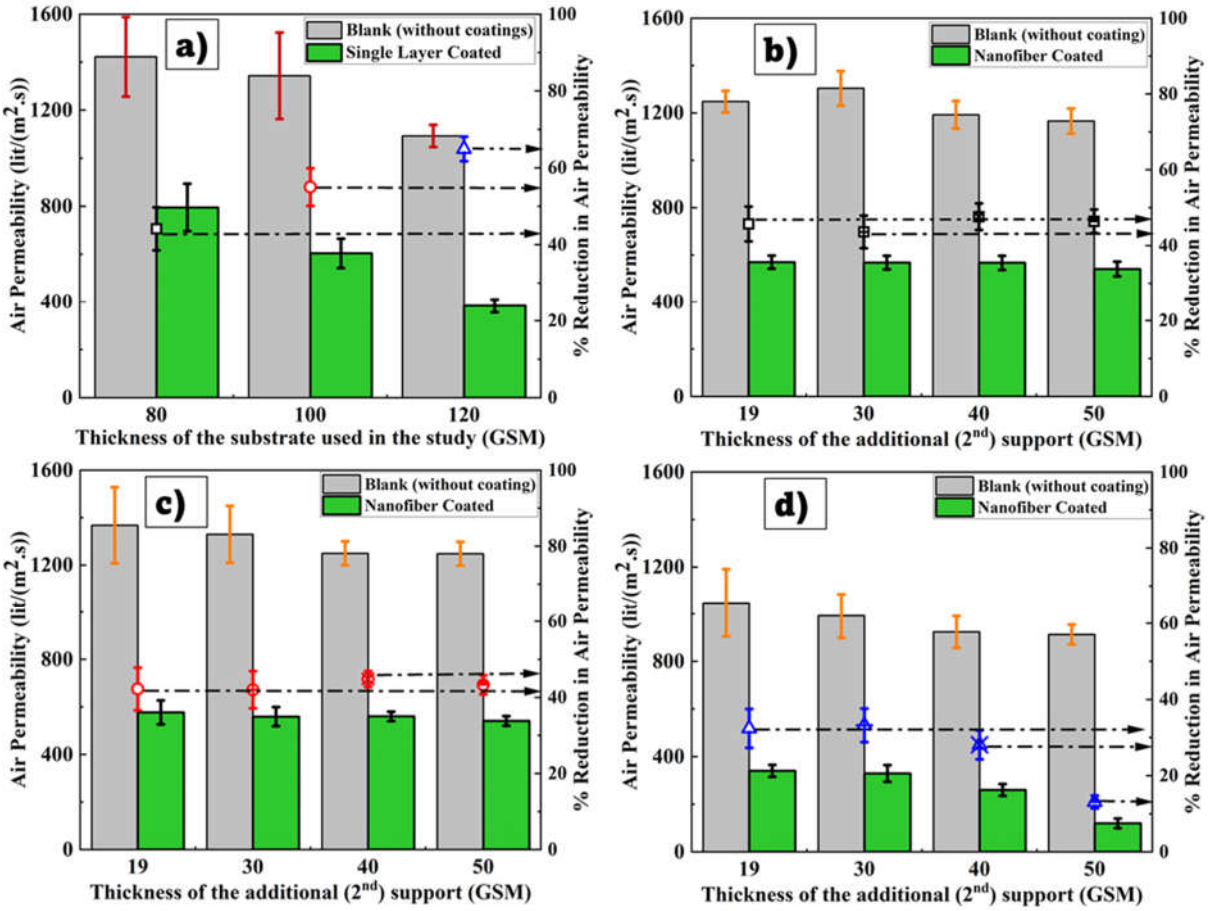

Figure 4 Presents the effect of nanofiber coating on air permeability in two-layer filtration

Base Substrate (GSM)	Avg. Air Permeability of Blank Combination (L/m²/s)	Avg. Air Permeability of Coated Combination (L/m²/s)	Percent Reduction in Permeability (%)
80	1248 ± 45.4	569 ± 13.2	54.4
100	1301 ± 72.8	559 ± 14.5	57.0
120	969 ± 58.0	262 ± 93.3	72.9

Table 2 effect of nanofiber coating on air permeability in two-layer filtration

Figure 4 presents the effect of nanofiber coating on air permeability in two-layer filtration configurations. Panel (a) shows single-layer-coated base substrates of varying GSM (80, 100, 120), while panels (b–d) depict configurations where these substrates are paired with an additional second support of different GSM (19, 30, 40, 50). For the two-layer configuration,

the addition of the second support layer significantly influences air permeability reduction. The base substrate alone (Figure 4a) exhibited percent reductions of 54.4%, 57.0%, and 72.9% for 80, 100, and 120 GSM respectively, indicating that thicker substrates inherently have lower initial permeability and experience higher proportional reductions upon nanofiber coating. In the two-layer system (Figures 4b–d), the air permeability dropped further compared to the single-layer setup due to the combined flow resistance of both layers and the nanofiber mat. However, as the GSM of the second support increased, the additional drop in permeability was relatively modest, suggesting that beyond a certain thickness, the second layer's contribution to resistance plateaus. This behavior reflects the balance between substrate porosity, coating density, and total layer thickness, where nanofiber coating remains the primary driver of permeability reduction in thicker assemblies.

The observed permeability reduction can be attributed to the formation of a dense, microporous nanofiber network over the substrate surface, as confirmed by SEM micrographs. This layer effectively decreases the mean pore size and increases the tortuosity of the airflow path, thereby enhancing the mechanical interception and diffusion of airborne particles(Podgórski et al., 2006). The effect was more pronounced in the 120 GSM substrates, where the combination of dense base media and the nanofiber layer produced the greatest reduction in permeability. Similar findings have been reported in previous studies where nanofiber coatings improved filtration efficiency at the expense of air permeability (Leung & Sun, 2020), underscoring the trade-off between particle capture and pressure drop in fibrous filter media.

4.3. General Discussion and Practical Implications

The observed trends align closely with established fibrous filtration theory. Electrospun nanofibers, with their diameters in the sub-micrometer to nanometer range, form a dense web with extremely small pore sizes and a very high specific surface area(Podgórski et al., 2006). This morphology enhances filtration efficiency by increasing the probability of particle capture through mechanisms such as interception, Brownian diffusion, and inertial impaction (Ahn et al., 2006)). In particular, for particles below ~0.3 μm, Brownian diffusion is dominant, while for larger particles, interception and impaction contribute significantly. However, this improved particle capture comes at the expense of airflow resistance. The addition of the nanofiber layer reduces the mean pore size and increases path tortuosity, leading to a decrease in permeability and an increase in pressure drop, in agreement with Darcy's law and Kozeny–Carman relationships for flow through porous media (Qin & Wang, 2006). The inverse relationship

between air permeability and pressure drop, observed in our results, is well-documented in filtration literature (Owens et al., n.d.).

In HVAC systems, elevated pressure drop translates into higher fan energy consumption (Y. Li & O'Neill, 2018). Therefore, filters must meet ISO 16890 or MERV rating requirements while maintaining minimal airflow resistance. Our data indicate that nanofiber coatings can achieve substantial performance gains with only a moderate pressure penalty, making them suitable for energy-conscious systems. In respiratory protection devices, user comfort depends heavily on low breathing resistance. Previous studies have shown that electrospun nanofiber layers can improve particle capture in N95-type respirators while keeping inhalation resistance within regulatory limits(Landim et al., 2023).

Our experimental methodology ensured statistical reliability: measurements were replicated (n=6 for single-layer, n=4 for two-layer) across different sample regions to account for local structural variability. The percentage change was calculated using the standard formulas:

- Percent Reduction: [(Value_Blank - Value_Coated) / Value_Blank] * 100
- Percent Increase: [(Value_Coated - Value_Blank) / Value_Blank] * 100

The relatively low standard deviations observed in both single- and two-layer configurations indicate consistent nanofiber deposition and reproducible filtration performance, similar to the reproducibility metrics reported in other electrospinning-based filter studies (Kasoju & Ye, 2021)).

5. Conclusion

This study has successfully demonstrated the fabrication and thorough evaluation of a high-performance composite air-filter medium, produced by coating a PET bicomponent spunbond substrate with polyamide-6 (PA6) and polyvinylidene fluoride (PVDF) nanofibres using a scalable needleless electrospinning technique. The work offers valuable insights into how the engineered microstructure of a filter influences its aerodynamic behaviour.

The principal findings involve a uniform, defect-free nanofibre layer with tightly controlled fibre diameters (averaging 150–180 nm) was deposited onto the nonwoven substrate. Scanning electron microscopy confirmed the formation of a dense, microporous surface structure, ideally suited for enhanced particulate capture. As anticipated, the addition of the nanofibre coating led to substantial reductions in air permeability (44–73 %) and corresponding increases in

pressure drop (ranging from 79 % to over 340 % in multi-layer configurations). These changes arise directly from the denser fibre packing and reduced pore size of the coated media. Further, the results clearly confirm the well-established compromise in fibrous filter design namely, that the microstructural features needed for high filtration efficiency (fine fibres and high packing density) inevitably lead to greater airflow resistance. This work quantifies the magnitude of these effects across substrates of varying weights and layer configurations, providing a robust dataset for future engineering applications. In summary, nanofibre coatings represent a highly effective means of upgrading conventional nonwoven media into high-performance filtration materials, offering particle removal capabilities far exceeding those of the base substrate. Nevertheless, this improvement is accompanied by reduced breathability and increased energy demand, as evidenced by the higher pressure drops measured.

The practical challenge, therefore, lies in optimising the nanofibre layer's thickness, density, and fibre diameter to meet the required filtration standard (e.g. HEPA or MERV) while maintaining an acceptable pressure drop for the intended application—whether in energy-efficient HVAC systems or in respirators where user comfort is paramount. This study provides a strong experimental foundation and detailed performance data to guide such optimisation in next-generation air-filter development.

6. References

Ahn, Y. C., Park, S. K., Kim, G. T., Hwang, Y. J., Lee, C. G., Shin, H. S., & Lee, J. K. (2006). Development of high efficiency nanofilters made of nanofibers. *Current Applied Physics*, *6*(6), 1030–1035. https://doi.org/10.1016/J.CAP.2005.07.013

Aruchamy, K., Mahto, A., Nano-Objects, S. N.-N.-S. &, & 2018, undefined. (n.d.). Electrospun nanofibers, nanocomposites and characterization of art: Insight on establishing fibers as product. *Elsevier*. Retrieved August 13, 2025, from https://www.sciencedirect.com/science/article/pii/S2352507X1830026X

Bhardwaj, N., advances, S. K.-B., & 2010, undefined. (2010). Electrospinning: A fascinating fiber fabrication technique. *ElsevierN Bhardwaj, SC KunduBiotechnology Advances, 2010•Elsevier*, *28*, 325–347. https://doi.org/10.1016/j.biotechadv.2010.01.004

Bokka, S. (2022). *Fabrication of Charged Fibrous Structures and their Applications in the Filtration and Separations*.

https://search.proquest.com/openview/2945510de1abce47bde497e70a347489/1?pq-origsite=gscholar&cbl=18750&diss=y

Casasola, R., Thomas, N. L., & Georgiadou, S. (2016). Electrospinning of poly (lactic acid): Theoretical approach for the solvent selection to produce defect-free nanofibers. *Wiley Online LibraryR Casasola, NL Thomas, S GeorgiadouJournal of Polymer Science Part B: Polymer Physics, 2016•Wiley Online Library*, *54*(15), 1483–1498. https://doi.org/10.1002/POLB.24042

Chidchanok Mit-uppatham, M. N. (n.d.). *Electrospun Polyamide-6 Nanofibers: Effects of Solvent Systems*. Retrieved August 12, 2025, from http://trimen.pl/witek/ciecze/old_liquids.html

Cho, Y., Beak, J. W., Sagong, M., Ahn, S., Nam, J. S., & Kim, I. D. (2025). Electrospinning and Nanofiber Technology: Fundamentals, Innovations, and Applications. *Advanced Materials*, *37*(28), 2500162. https://doi.org/10.1002/ADMA.202500162;REQUESTEDJOURNAL:JOURNAL:15214095;WGROUP:STRING:PUBLICATION

Cohen, A. J., Brauer, M., Burnett, R., Anderson, H. R., Frostad, J., Estep, K., Balakrishnan, K., Brunekreef, B., Dandona, L., Dandona, R., Feigin, V., Freedman, G., Hubbell, B., Jobling, A., Kan, H., Knibbs, L., Liu, Y., Martin, R., Morawska, L., … Forouzanfar, M. H. (2017). Estimates and 25-year trends of the global burden of disease attributable to ambient air pollution: an analysis of data from the Global Burden of Diseases Study 2015. *The Lancet*, *389*(10082), 1907–1918. https://doi.org/10.1016/S0140-6736(17)30505-6

Deitzel, J. M., Kleinmeyer, J., Harris, D., & Beck Tan, N. C. (2001). The effect of processing variables on the morphology of electrospun nanofibers and textiles. *Polymer*, *42*(1), 261–272. https://doi.org/10.1016/S0032-3861(00)00250-0

Gibson, P., Schreuder-Gibson, H., & Rivin, D. (2001). Transport properties of porous membranes based on electrospun nanofibers. *Colloids and Surfaces A: Physicochemical and Engineering Aspects*, *187*(188), 469–481. https://doi.org/10.1016/S0927-7757(01)00616-1

Grasl, C., Arras, M. M. L., Stoiber, M., Bergmeister, H., & Schima, H. (2013). Electrodynamic control of the nanofiber alignment during electrospinning. *Applied Physics Letters*, *102*(5). https://doi.org/10.1063/1.4790632/1068431

Heng, Z., Xiaoming, Q., Qi, Z., & Zhaohang, Y. (2015). Research on structure characteristics and filtration performances of PET-PA6 hollow segmented-pie bicomponent spunbond nonwovens fibrillated by hydro entangle method. *Journal of Industrial Textiles*, *45*(1), 48–65. https://doi.org/10.1177/1528083714521073/ASSET/2B87719B-31DA-4E12-A30C-B7609A37D707/ASSETS/IMAGES/LARGE/10.1177_1528083714521073-FIG8.JPG

Huang, J. J., Tian, Y., Wang, R., Tian, M., & Liao, Y. (2020). Fabrication of bead-on-string polyacrylonitrile nanofibrous air filters with superior filtration efficiency and ultralow pressure drop. *Separation and Purification Technology*, *237*, 116377. https://doi.org/10.1016/J.SEPPUR.2019.116377

Kasoju, N., & Ye, H. (2021). *Biomedical Applications of Electrospinning and Electrospraying*. https://books.google.com/books?hl=en&lr=&id=InINEAAAQBAJ&oi=fnd&pg=PP1&dq=nanofiber+deposition+and+reproducible+filtration+performance,+similar+to+the+reproducibility+metrics+reported+in+other+electrospinning-based+filter+studies+(Moghadam+et+al.,+2020).&ots=cd3gS3w351&sig=dQN7Gt6R6enmrcOgyH-NHoyaUkg

Khawar, M. T., Gong, H., Zia, Q., Nawaz, H. H., & Li, J. (2023). Effect of Low-Pressure Plasma Surface Modification on Filtration Performance of Chitosan Nanofibrous Respiratory Filter. *Fibers and Polymers*, *24*(3), 947–958. https://doi.org/10.1007/S12221-023-00029-7/FIGURES/17

Kumar, A., Malyan, V., & Sahu, M. (2023). Air pollution control technologies for indoor particulate matter pollution: a review. *Springer*, *7*(2), 261–282. https://doi.org/10.1007/S41810-023-00178-5

Landim, M. G., Carneiro, M. L. B., Joanitti, G. A., Anflor, C. T. M., Marinho, D. D., Rodrigues, J. F. B., de Sousa, W. J. B., Fernandes, D. de O., Souza, B. F., Ombredane, A. S., do Nascimento, J. C. F., Felice, G. de J., Kubota, A. M. A., Barbosa, J. S. C., Ohno, J. H., Amoah, S. K. S., Pena, L. J., Luz, G. V. da S., de Andrade, L. R., … Rosa, S. de S. R.

F. (2023). A novel N95 respirator with chitosan nanoparticles: mechanical, antiviral, microbiological and cytotoxicity evaluations. *Discover Nano*, *18*(1), 1–21. https://doi.org/10.1186/S11671-023-03892-8/METRICS

Leung, W. W. F., & Sun, Q. (2020). Charged PVDF multilayer nanofiber filter in filtering simulated airborne novel coronavirus (COVID-19) using ambient nano-aerosols. *Separation and Purification Technology*, *245*, 116887. https://doi.org/10.1016/J.SEPPUR.2020.116887

Li, P., Wang, C., Zhang, Y., & Wei, F. (2014). Air filtration in the free molecular flow regime: a review of high-efficiency particulate air filters based on carbon nanotubes. *Wiley Online Library*, *10*(22), 4543–4561. https://doi.org/10.1002/SMLL.201401553

Li, X., Li, J., Li, K., Zhang, S., Yang, Z., Zhang, C., Zhang, J., Li, Y., Zhang, D., Liu, Y., & Hu, X. (2025). From Fiber to Power: Recent Advances Toward Electrospun-Based Nanogenerators. *Advanced Functional Materials*, *35*(13), 2418066. https://doi.org/10.1002/ADFM.202418066

Li, Y., & O'Neill, Z. (2018). A critical review of fault modeling of HVAC systems in buildings. *Building Simulation*, *11*(5), 953–975. https://doi.org/10.1007/S12273-018-0458-4/METRICS

Luo, X., Wang, J., Zhang, P., Feng, J., Meng, X., … K. L.-S. and, & 2024, undefined. (n.d.). "Rooting" engineering strategy for construction of highly stable, scalable, size-customized oxidized graphene/PA6 ultrafine fiber composite nanofiltration membranes. *Elsevier*. Retrieved August 12, 2025, from https://www.sciencedirect.com/science/article/pii/S2468023024000385

Motamedi, A. S., Mirzadeh, H., Hajiesmaeilbaigi, F., Bagheri-Khoulenjani, S., & Shokrgozar, M. A. (2017a). Effect of electrospinning parameters on morphological properties of PVDF nanofibrous scaffolds. *Progress in Biomaterials*, *6*(3), 113. https://doi.org/10.1007/S40204-017-0071-0

Motamedi, A. S., Mirzadeh, H., Hajiesmaeilbaigi, F., Bagheri-Khoulenjani, S., & Shokrgozar, M. A. (2017b). Effect of electrospinning parameters on morphological properties of PVDF nanofibrous scaffolds. *Progress in Biomaterials*, *6*(3), 113–123. https://doi.org/10.1007/S40204-017-0071-0/FIGURES/10

Owens, L., BioResources, M. H.-, & 2023, undefined. (n.d.). Performance Factors for Filtration of Air Using Cellulosic Fiber-based Media: A Review. *Search.Ebscohost.Com*. Retrieved August 13, 2025, from https://search.ebscohost.com/login.aspx?direct=true&profile=ehost&scope=site&authtype=crawler&jrnl=19302126&AN=161659549&h=OOOvsMYhrtP5g5uOPHnSw9gXRBhf33cE%2Bqdu76oQgl2hih2cZndJFqM9mtDIl0DpShdCECZ2MUyL7vU8W0LzWw%3D%3D&crl=c

Podgórski, A., Bałazy, A., & Gradoń, L. (2006). Application of nanofibers to improve the filtration efficiency of the most penetrating aerosol particles in fibrous filters. *Chemical Engineering Science*, *61*(20), 6804–6815. https://doi.org/10.1016/J.CES.2006.07.022

Qin, X. H., & Wang, S. Y. (2006). Filtration properties of electrospinning nanofibers. *Journal of Applied Polymer Science*, *102*(2), 1285–1290. https://doi.org/10.1002/APP.24361;WGROUP:STRING:PUBLICATION

Reneker, D. H., & Yarin, A. L. (2008). Electrospinning jets and polymer nanofibers. *Polymer*, *49*(10), 2387–2425. https://doi.org/10.1016/J.POLYMER.2008.02.002

Sanyal, A., Polymers, S. S.-R.-, & 2021, undefined. (n.d.). Ultrafine PVDF nanofibers for filtration of air-borne particulate matters: A comprehensive review. *Mdpi.Com*. Retrieved August 12, 2025, from https://www.mdpi.com/2073-4360/13/11/1864

Sanyal, A., & Sinha-Ray, S. (2021). Ultrafine PVDF Nanofibers for Filtration of Air-Borne Particulate Matters: A Comprehensive Review. *Polymers 2021, Vol. 13, Page 1864*, *13*(11), 1864. https://doi.org/10.3390/POLYM13111864

Schneider, C., Rasband, W., methods, K. E.-N., & 2012, undefined. (n.d.). NIH Image to ImageJ: 25 years of image analysis. *Nature.ComCA Schneider, WS Rasband, KW EliceiriNature Methods, 2012•nature.Com*. Retrieved August 13, 2025, from https://idp.nature.com/authorize/casa?redirect_uri=https://www.nature.com/articles/nmeth.2089&casa_token=uSVoImbU77kAAAAA:37OvAafVF0amiMN8sKU-Eh4w19l2ai7v5ugOAF4p2dWgaa43bBHyNhLw6q3tSfecDTEuVDTB0cVKVAioV4Y

Science, M. C.-J. of A. P., & 2025, undefined. (2025). Performance Comparison of PVDF-Based Unimodal and Bimodal Electret Air Filters via Solution-Blowing and Electro-Blowing Methods. *Wiley Online Library*, *142*(19). https://doi.org/10.1002/APP.56855

Sedar, E. (2025). *Improved Production of Polymer Nanofibers via High Speed Centrifugal Spinning*. https://search.proquest.com/openview/3606c79ada8ec0e9fe0376a4923603a9/1?pq-origsite=gscholar&cbl=18750&diss=y

Singh, S., Vishwakarma, P., & Gupta, T. (2024). Review of current and future indoor air purifying technologies. *ACS Publications*, *4*(11), 2607–2630. https://doi.org/10.1021/ACSESTENGG.4C00460

Širc, J., Hobzová, R., Kostina, N., Munzarová, M., Juklíčková, M., Lhotka, M., Kubinová, Š., Zajícová, A., & Michálek, J. (2012). Morphological Characterization of Nanofibers: Methods and Application in Practice. *Journal of Nanomaterials*, *2012*(1), 327369. https://doi.org/10.1155/2012/327369

Teo, W. E., & Ramakrishna, S. (2006). A review on electrospinning design and nanofibre assemblies. *Nanotechnology*, *17*(14). https://doi.org/10.1088/0957-4484/17/14/R01,

Venkataraman, D. (2024). *NANOFIBER FILTER PERFORMANCE : SYSTEMIC STUDY ON EFFICIENCY, REUSABILITY, PROTECTION AND BREATHABILITY A DISSERTATION PRESENTED*.

Yu, M., Dong, R. H., Yan, X., Yu, G. F., You, M. H., Ning, X., & Long, Y. Z. (2017). Recent Advances in Needleless Electrospinning of Ultrathin Fibers: From Academia to Industrial Production. *Macromolecular Materials and Engineering*, *302*(7). https://doi.org/10.1002/MAME.201700002

Zhu, M., Han, J., Wang, F., Shao, W., Xiong, R., Zhang, Q., Pan, H., Yang, Y., Samal, S. K., Zhang, F., & Huang, C. (2017). Electrospun nanofibers membranes for effective air filtration. *Wiley Online Library*, *302*(1). https://doi.org/10.1002/MAME.201600353